Developmental Biology **234,** 441–453 (2001)
doi:10.1006/dbio.2001.0255, available online at http://www.idealibrary.com on IDEAL®

Tantalus, a Novel ASX-Interacting Protein with Tissue-Specific Functions

Bruce H. Dietrich,* Jocelyn Moore,† Michael Kyba,† Gilbert dosSantos,* Fiona McCloskey,* Thomas A. Milne,† Hugh W. Brock,† Henry M. Krause*,[1]

**Banting and Best Department of Medical Research, Department of Molecular and Medical Genetics, University of Toronto, Charles H. Best Institute, 112 College Street, Toronto, Ontario, Canada, M5G 1L6; and †Department of Zoology, University of British Columbia, 6270 University Boulevard, Vancouver, British Columbia, Canada, V6T 1Z4*

The *Drosophila* trithorax- and Polycomb-group (trxG and PcG) proteins maintain activated and repressed transcriptional states at specific target gene loci. The *Additional sex combs* (*Asx*) gene is of particular interest as it appears to function in both protein complexes and yet its effects on target genes are more restricted. A novel protein, Tantalus (TAN), was identified in a yeast two-hybrid screen for ASX-interacting proteins that might confer tissue-specific ASX functions. TAN contains consensus nuclear localization sites and binds DNA *in vitro*. However, its subcellular localization varies in a tissue-specific fashion. In salivary glands, TAN is predominantly nuclear and associates with 66 euchromatic sites on polytene chromosomes, more than half of which overlap with ASX. These loci do not include the homeotic genes of the ANT and BX complexes bound by other PcG and trxG proteins. Rather, *tan* mutant defects are restricted to sensory organs. We show that one of these defects, shared by *Asx*, is genetically enhanced by *Asx*. Taken together, the data suggest that TAN is a tissue-specific cofactor for ASX, and that its activity may be partially controlled by subcellular trafficking. © 2001 Academic Press

Key Words: **Additional sex combs; *tantalus*; tissue-specific; trithorax; Polycomb; *Drosophila*; sensory organs.**

INTRODUCTION

Differentiation in higher organisms requires that cells maintain activated or repressed transcriptional states at specific loci for extended periods of development. Two highly conserved protein complexes play a major role in these regulatory processes: Polycomb-group (PcG) protein complexes act to maintain states of transcriptional repression, while trithorax-group (trxG) protein complexes act to maintain states of transcriptional activation (reviewed in Jacobs and van Lohuizen, 1999). Mutations in PcG genes cause posteriorly directed transformations in embryos and adults due to a failure to maintain the repressed states of genes within homeobox gene complexes (referred to collectively as HOM-C) (Simon, 1995). Conversely, mutations in trxG genes result in anteriorly directed transformations due to a failure to maintain the active transcriptional states of HOM-C genes (reviewed in Kennison, 1995). Since their initial characterization as regulators of HOM-C genes, trxG and PcG genes have also been shown to regulate many other developmental processes including specification of the CNS and PNS, dorsal—ventral patterning, imaginal disc growth, and segmentation (see Simon, 1995 and references therein).

Approximately 15 PcG proteins have been identified functionally and as many as 30–40 are predicted to exist (Jürgens, 1985; Landecker *et al.*, 1994). PcG proteins interact physically (Franke *et al.*, 1992; Strutt and Paro, 1997; Peterson *et al.*, 1997; Kyba and Brock, 1998; Jones *et al.*, 1998; Tie *et al.*, 1998; Shao *et al.*, 1999), suggesting that they form large multiprotein complexes *in vivo*. These complexes are thought to maintain repressed transcriptional states by organizing transcriptionally inaccessible chromatin conformations (Paro, 1990). Most identified PcG proteins bind numerous euchromatic sites on polytene chromosomes, including sites for the well-characterized Antennapedia and Bithorax complexes (ANT-C and BX-C)

[1] To whom correspondence should be addressed. Fax: 416-978-8528. E-mail: h.krause@utoronto.ca.

0012-1606/01 $35.00

(Zink and Paro, 1989; DeCamillis *et al.*, 1992; Franke *et al.*, 1992; Martin and Adler, 1993; Rastelli *et al.*, 1993; Lonie *et al.*, 1994; Peterson *et al.*, 1997; Sinclair *et al.*, 1998a). Interestingly, the composition of complexes formed at non-HOM-C chromosomal sites varies (see Rastelli *et al.*, 1993; Sinclair *et al.*, 1998a), suggesting that different complexes are required to regulate other PcG target genes.

As with the PcG proteins, trxG proteins are believed to associate as multiprotein complexes, but act by maintaining target gene loci in accessible conformations (Dingwall *et al.*, 1995; Papoulas *et al.*, 1998; Collins *et al.*, 1999; Crosby *et al.*, 1999; Kal *et al.*, 2000). The majority of trxG genes were identified by screening for dominant suppressors of PcG phenotypes (Kennison and Tamkun, 1988), suggesting that there is a close functional and physical relationship between the two types of protein complexes.

The *Additional sex combs* (*Asx*) gene was initially classified as a PcG gene. Zygotic mutations were first shown to affect larval head development (Nüsslein-Volhard *et al.*, 1984) and subsequently to enhance other PcG gene phenotypes (Jürgens, 1985; Campbell *et al.*, 1995). Although transformations caused by zygotic *Asx* mutations are weaker than those seen in other *Pc* mutants (Breen and Duncan, 1986), *Asx* mutants do cause ectopic derepression of HOM-C genes (McKeon and Brock, 1991; Simon *et al.*, 1992; Soto *et al.*, 1995). As heterozygotes, *Asx* adults also exhibit typical PcG-like homeotic transformations including occasional ectopic sex combs on T2 legs in males and the transformation of A4 tergites into A5 tergites. Heterozygous adults and homozygous embryos also exhibit segmentation defects (Sinclair *et al.*, 1992).

The relatively weak nature of *Asx* homozygous phenotypes may be partially explained by evidence suggesting that ASX also plays a role in trxG function. For example, a P-element induced allele of *Asx*, Asx^{P1}, exhibits both anterior and posterior transformations (Sinclair *et al.*, 1992). Second, several *Asx* alleles, including a deficiency, enhance the thoracic and abdominal defects of the trxG gene *trithorax* (*trx*) (Milne *et al.*, 1999). Finally, *Asx* mutations enhance position—effect–variegation, a result not expected for a PcG member (Sinclair *et al.*, 1998b). ASX is not the first protein suggested to have both PcG and trxG activities: the *Enhancer of zeste* gene was originally identified as a PcG gene, but has since been shown to have trxG activity (LaJeunesse and Shearn, 1996). More recently, alleles of several genes previously characterized as PcG genes were shown to be genetic enhancers of both trxG and PcG loci (Gildea *et al.*, 2000). These results have prompted the designation of an additional gene class, the enhancers of *trithorax* and *Polycomb* mutations, or ETP class.

One of the main unanswered questions in trxG/PcG research is how these proteins are recruited and assembled on target gene promoters. For example, although ASX is expressed ubiquitously during early development (Sinclair *et al.*, 1998a), *Asx* mutations cause extensive derepression of HOM-C genes in the epidermis and visceral mesoderm but not in the central nervous system (CNS) (Simon *et al.*, 1992; Soto *et al.*, 1995). Interestingly, although *Asx* mutations have little effect on *Ubx* expression in the CNS (Soto *et al.*, 1995; Sinclair *et al.*, 1988a), a reporter construct attached to a 14.5-kb *Ubx* enhancer element (*bxd14*) is completely derepressed in the CNS of ASX mutants (Soto *et al.*, 1995). Thus, ASX is functional in the CNS, but appears to require specific cofactors to regulate particular regulatory elements. Other cofactors are likely required to facilitate other tissue- and promoter-specific functions.

In order to identify ASX-specific cofactors, a yeast two-hybrid screen using ASX as bait was initiated. A novel DNA binding protein that we refer to as Tantalus (TAN) was identified. TAN also associates with ASX in GST pull-down experiments, and colocalizes with ASX at a subset of ASX polytene chromosome binding sites. We also show that *Asx* and *tan* interact genetically. Interestingly, TAN is unlike other trxG/PcG complex components in that it exhibits differential subcellular localization, and it appears to play no role in regulating HOM-C gene expression. Rather, TAN appears to be a novel cofactor for ASX that specifically facilitates roles in sensory organ development.

MATERIALS AND METHODS

Molecular Techniques

Cloning tan. The yeast two-hybrid screen has been described elsewhere (Kyba and Brock, 1998). Genomic and cDNA library screens, sequencing, and Northern/Southern blots were done according to standard procedures (Sambrook *et al.*, 1989).

GST pull-downs. Amino acids 1139–1668 of ASX were subcloned into pGEX4T1 (Amersham Pharmacia Biotech). GST beads were bound to GST and GST-ASX at a concentration of 2 μg/μl for GST and 0.4 μg/μl for GST-ASX. Beads were resuspended in an equal volume of 1× Binding Buffer 1 (1× BB1: 25 mM Hepes, pH 7.5, 5 mM KCl, 1 mM EDTA, 0.25 mM DTT, 0.05% Tween 20, 1 mg/ml BSA, 10% glycerol). The Promega TNT T7 Rabbit Reticulocyte Lysate System was used to synthesize full-length TAN (25-μl reaction) which was passed over a Sephadex G-25 column and diluted to 100 μl with 1× BB1. The probe was incubated at 4°C for 30 min to block and then 50 μl added to each of the GST and GST-ASX beads (total volume is 100 μl). Reactions were incubated at 4°C with mixing for 2 h and then washed two times with 1× BB1 and two times with Wash Buffer (20 mM Hepes, pH 7.5, 0.15 M NaCl, 10% glycerol). Bound probe was eluted with 15 μl of 1× SDS buffer and analyzed by SDS–PAGE.

In situ hybridization. RNA probes were prepared as described previously (Hughes and Krause, 1999), except that secondary antibodies were HRP conjugated and the ABC system of PIERCE was used for detection.

tan and p53-tan constructs. The tan cDNA was subcloned into the vector pET19b (Novagen) for T7 expression and the *hsp*70 vector pCaSpeR (Thummel and Pirrotta, 1992) or UAS vector pUAST (Brand and Perrimon, 1993) for *in vivo* expression. Transgenic lines were created by using standard techniques. The p53 tag was inserted at a *Bst*EII site of the *tan* cDNA (located at amino acid 19). The inserted sequence is N-RSRAFRHSVV-R (new sequence between dashes). The rescue construct is approximately 7 kb in size consisting of 1477-bp upstream of *tan* (a *Bam*HI site) and 3-kb downstream of *tan* (a *Sal*I site) cloned into pW8 (Klemenz *et al.*,

1987). Flies were made homozygous for both the rescue construct and tan^2 deletion (P[*tan*]/P[*tan*];tan^2/tan^2).

TAN DNA binding experiment. Five micrograms of sonicated salmon sperm DNA was vacuum blotted to nitrocellulose (nitrocellulose gave less background then other membranes) in a 30-μl mixture of DNA and 2× SSC followed by a wash in 500 μl 2× SSC. The blot was blocked with 1× Binding Buffer 2 (1× BB2: 2% milk powder, 20 mM Tris, pH 7.6, 100 mM NaCl, 0.25 mM EDTA, 0.25 mM DTT, 0.1% Tween 20, and 10% glycerol) for 2 h on ice. Radioactively labeled proteins were synthesized by using the Promega TNT T7 kit and incubated with the blots in 1× BB2 for 25 min on ice. Blots were washed with 1× BB2 with several changes over 15 min, dried, and exposed to film.

Antibodies. Either full-length TAN or residues 87–164 were fused to GST and purified for injection into rabbits (GST-TAN was partially degraded, therefore the largest stable band was used for injection). Antibodies were purified as described (Sinclair *et al.*, 1998a) with both antibodies giving similar results. Kc extracts were made as described previously (Kyba and Brock, 1998). Polytene chromosomes were stained as described (Sinclair *et al.*, 1998a) with a 1/75 dilution of affinity purified anti-TAN antibody. Serum depleted by passage over columns containing GST-TAN did not react with polytene chromosomes, demonstrating the specificity of the antibody. Double-staining of polytene chromosomes was undertaken with the sheep anti-ASX antibody described previously (Sinclair *et al.*, 1998a) and the rabbit anti-TAN antibody described here. Binding was detected with appropriate secondary antibodies labeled with Alexa Fluor 488 (Molecular Probes) and Cy3 (Jackson Laboratories). To immunostain imaginal discs, larvae were dissected and fixed as described (Hughes and Krause, 1999). Fixed tissues were dehydrated by using several changes of methanol followed by washes in PBST (1× PBS + 0.3% Triton X-100). Tissues were blocked in PBST + 0.5% BSA for 2.5 h. Tissues were incubated overnight at 4°C in appropriate antibodies [1/50 dilution of a monoclonal anti-p53 antibody (Santa Cruz Biotechnology, Inc.) or 1/500 dilution of anti-TAN against full-length TAN] in 1× PBS + 0.5% BSA. Tissues were washed quickly several times followed by 3× 30-min washes in PBST + 0.5% BSA. Tissues were incubated in secondary antibodies for 45 min [1/300 anti-mouse HRP (Bio-Rad) or 1/300 anti-rabbit Alexa Fluor 488 (Molecular Probes)] followed by washes in PBT for 1 h. For fluorescent staining, tissues were incubated in propidium iodide to stain nuclei. The HRP staining was developed by using the ABC system of Pierce. After staining, HRP tissues were washed in PBS and a glycerol solution (50:50 with 1× PBS), while fluorescent tissues were washed in 70% glycerol/2% DABCO, before dissection and mounting.

P-Element Screen

The screen was performed based on the protocol of Hamilton and Zinn (1994). Lines 0545/01, 0666/10, and 1203/07 from Deák and coworkers (1997) were used for the P-element mutagenesis screen. Groups of 20 flies containing hopped P-elements were analyzed by PCR using the P-element inverted repeat sequence as a primer and several primers from the *tan* genomic sequence (sequences available upon request). One line was obtained from 0545/01 that contained an insert in *tan* (see Fig. 2A). The 0545/01 line contains a lethal mutation located outside of the 65A region which was recombined off the chromosome to make homozygously viable tan^1/tan^1 flies. A similar procedure was used to screen for deletions of *tan* after hopping the P-element from the gene.

Drosophila Strains, Crosses, and Analysis

Asx^3, Asx^9, Asx^{15}, and Df(2R)*trix* (deletion of 51A1–2 to 51B6) have been described (Sinclair *et al.*, 1992), and the wild-type strain used is Oregon-R. Crosses for genetic analysis were 15–20 males and females mated for 3–4 days. Parents were either transferred to new bottles or dumped and progeny allowed to hatch until Day 17 for counting (parents are introduced to bottles at Day 0). Tissue samples were prepared as described (Sinclair *et al.*, 1992). *engrailed*-GAL4, *patched*-GAL4, *hairy*-GAL4, and C96-GAL4 are described in Flybase (http://flybase.bio.indiana.edu:82).

RESULTS

Identifying Novel ASX Cofactors

The *Asx* protein contains 1668 amino acids (Sinclair *et al.*, 1998a). The C-terminal 500 amino acids constitute the main region of homology to mammalian counterparts (E. O'Dor and H.W.B., unpublished results), and include a cysteine cluster with 25 of 28 residues conserved. As most conserved PcG protein domains are required for protein–protein interactions (Peterson *et al.*, 1997; Gunster *et al.*, 1997; Kyba and Brock, 1998; Hashimoto *et al.*, 1998), this region (residues 1139–1668) was used to make a yeast two-hybrid bait construct. A 0- to 12-h embryonic cDNA library was screened, and out of approximately 10^5 clones, 11 unique interacting constructs were recovered (data not shown). One of these, which we have subsequently named *tantalus* (*tan*), is described here. The *tan* clone did not interact with control constructs, nor did it interact with 23 of 24 two-hybrid baits constructed from 11 PcG or PcG-related proteins. The function of the latter interaction will be addressed elsewhere.

To verify the two-hybrid interaction between ASX and TAN, a GST pull-down assay was employed. Residues 1139–1668 of ASX were used to make a GST-ASX fusion protein. GST and GST-ASX were purified and bound to glutathione beads. The two resins were then incubated with ^{35}S-labeled TAN produced using a reticulocyte lysate. ^{35}S-TAN was not precipitated by GST, but was efficiently pulled down by the GST-ASX fusion protein (Fig. 1). Based on the yeast two-hybrid and GST pull-down results, we conclude that ASX and TAN are likely to interact directly.

Characterization of the tan Gene

Two overlapping *tan* cDNAs were recovered from an embryonic cDNA library. The combined sequence suggests a full-length transcript of approximately 1.6 kb, which is consistent with the size of transcripts identified by Northern blotting (see below). Approximately 7 kb of genomic DNA flanking the cDNA sequence was obtained and 4 kb surrounding the *tan* locus was sequenced (Fig. 2A). The genomic sequence contains two introns, one within the

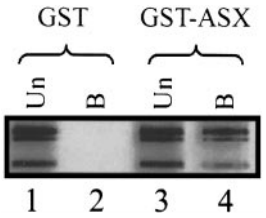

FIG. 1. GST pull-down experiments. Labeled TAN was incubated with GST or GST-ASX and the unbound (5% of sample) and bound (100% of sample) fractions were analyzed by SDS–PAGE. Unbound (Un) (Lanes 1 and 3) and Bound (B) (Lanes 2 and 4) fractions of TAN from GST (Lanes 1 and 2) and GST-ASX (Lanes 3 and 4) samples are shown. The two faster migrating bands most likely result from alternate translational start sites. The interaction of the fastest migrating band with ASX appeared to be weaker than full-length protein (compare right two lanes), and may uncover part of an ASX interaction domain in TAN.

coding region and the second located upstream of the putative ATG translational start site. This ATG conforms well to consensus translation start sites (Cavener, 1987) and yields a protein with a predicted mass of 33 kDa.

TAN lacks homology to any of the proteins currently listed in GenBank, but does contain several regions of interest (Fig. 2B). Two large basic regions consisting of 32% (21/66) and 41% (19/46) basic amino acids are located at residues 90–154 and 188–235. Despite these large basic patches, the overall p*I* predicted for TAN is 6.4. The protein has two canonical nuclear localization signals at residues 90–106 (RRSSTFGARAGVARRRM) and 217–220 (KRRR). The protein also contains two potential PEST regions (Proline, Glutamate, Serine, and Threonine) which are believed to act as protein degradation signals (Rechsteiner and Rogers, 1996). Numerous

A

```
GCTTTATTAAATGTGCCACTTATTTTGAATATTCCGCAAAAATAGGTAATCGATAGCTGTTCATTTATCCGAAACTATCGGTTTTGGCTG
                                 ↱1          ▼                                ↱2        ↱3
AACCCAAGTACACTACCTATCGATACAATTGTGAGTGGTTGAACCAGCTCTAATCCAAGCTGTTTATTTTACAAAAAGAACACAAAAGTT
ATAATTCTGTCATTTAATTGTCTGCAAAATAGGCATTTCCAGCATCATTGCATGTAGTTAAATCCAGATTTCTGAAAAACCTTATTTGGC
AGCGATATGTTTAGCCTAAAAATAGGAATTTGCGGATAAATTACCCCCCGGAGTGACAAAGATCTGTATTGTCATACAGACGCCTGCAGA
AAAAAGGGTTTTACAAGAAGAAAATGCTCTATTTTGCAGAGGTTAGTAAACTTTAGGTAATCTTTGACTTCCAAGATCTCTAACTCGAGT
TACTTAGCAGTTCCGACGGCTTTAACTGATATCTTTGAGCTAAGATACAAGGAATAAACCTTTCAAAAAGATAACTAATATGTATGCTTT
                                                  M  D  N  I  V  Y  D  F  A  K  I  T  F  Q  14
CCGTTTGTTTACTGTTAGGAATGATTTCTAGAATTCAACGTCAAATATAATGGATAACATAGTCTACGACTTTGCCAAGATCACGTTTCA
 A  K  D  N  R                                                    S  P  T  T  N  S  N  26
AGCTAAAGACAACAGGTAGGCCTTTAGAATAATTTATATCTGAAACTAGCCCAAAATTCATACTTCAGGTCACCCACTACTAACTCGAAT
L  S  W  Q  L  N  Q  M  A  L  S  D  M  E  E  M  Q  D  T  S  E  P  I  A  P  P  E  S  D  D  56
CTGTCGTGGCAACTAAATCAGATGGCCTTGTCGGACATGGAGGAGATGCAGGACACATCCGAGCCCATAGCTCCACCCGAATCCGATGAC
N  V  S  S  E  S  H  D  S  D  D  V  D  S  Q  L  S  R  C  E  D  N  D  D  D  S  D  C  I  S  86
AATGTCAGCAGTGAATCGCAAGACTCCGACGATGTAGACTCGCAATTGAGTCGCTGCGAGGACAACGATGACGACAGCGATTGCATCAGT
G  S  S  R  R  S  S  T  F  G  A  R  A  G  V  A  R  R  R  M  P  A  R  V  S  K  D  N  F  N  116
GGATCCTCCAGACGCAGTTCCACTTTTGGAGCTCGAGCGGGCGTGGCTCGTCGCAGAATGCCCGCCAGGGTGTCCAAGGACAACTTTAAC
R  I  C  S  A  I  M  K  P  I  K  K  K  Q  R  K  E  L  N  T  N  A  Q  T  L  K  S  I  E  K  146
CGGATCTGCAGCGCCATCATGAAACCCATCAAAAAGAAGCAACGCAAAGAACTGAACACAAATGCCCAAACACTTAAAAGCATCGAAAAG
I  Y  T  S  R  R  M  K  K  F  T  P  T  N  L  E  T  I  F  E  E  P  S  D  E  N  A  A  D  A  176
ATCTACACCAGCAGGCGCATGAAAAAGTTCACGCCCACCAATCTGGAGACAATCTTCGAGGAACCCAGCGATGAGAATGCCGCCGATGCA
E  D  D  S  E  E  C  S  I  S  S  Q  V  K  V  V  K  V  W  G  R  K  L  R  R  A  I  S  F  S  206
GAGGACGACAGCGAAGAGTGCTCCATCAGCAGCCAAGTGAAAGTAGTTAAGGTGTGGGGTCGCAAACTCCGCCGGGCAATATCCTTCAGC
D  G  L  N  K  N  K  I  L  S  K  R  R  R  Q  K  V  K  K  T  F  G  K  R  F  A  L  K  K  I  236
GATGGCCTGAACAAGAACAAAATCCTGTCGAAGAGACGCCGCCAGAAGGTGAAGAAGACCTTTGGCAAGCGTTTCGCACTCAAGAAAATC
S  M  T  E  F  H  D  R  L  N  K  S  F  D  S  A  M  L  E  G  D  D  A  E  A  G  G  S  A  E  266
TCCATGACCGAGTTCCACGATCGTCTGAATAAGAGCTTCGACAGTGCCATGCTGGAGGGGGATGATGCAGAGGCGGGAGGATCGGCGGAG
A  V  N  I  P  K  T  S  M  T  M  E  D  I  Q  L  P  T  M  S  S  Q  H  Q  F  L  M  Q  P  A  296
GCCGTCAACATCCCCAAGACATCCATGACCATGGAAGACATACAGCTGCCGACAATGAGCAGCCAGCACCAGTTCCTCATGCAACCGGCG
G  F  E  *                                                                              299
GGCTTTGAGTAGAGAGACTGAATGATCCATCAAATACGCCCCACATTGATTTGCATTGCATTAAAACTAGCTAATAGTGCCCAAAAATAA
ATGTACTGATTACCAATTATGAAGTTAGGATTTACGTTCGTTTGGTTAACTTCTCACCTTAGTCTTAAGCCCCATAAAAGTTATAAATGA
GTGTAAATAGCATGTACAAGAAAAGAAAATAAGAGCTATACCTAGAGCTAAACTTATCCAGCCATAGAATACGATTCTGTGCTTAGCCAT
TAAGATAATAAATAAAAGTTGAAAATACATATCCATCCACTGTCGTTCGG
```

B

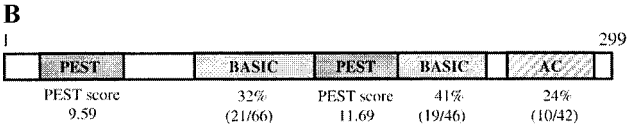

FIG. 2. Genomic and amino acid sequence of *tan*. (A) Sequence of the *tan* locus with introns (two boxed sequences) and putative polyadenylation signal (**AATAAA**) indicated. Arrows labeled 1, 2, and 3 denote the 5′ ends of the cDNAs identified by, respectively, our screen and two ESTs from the Berkeley EST project (Flybase). Also indicated is the transposon insert site from the P-element screen (arrowhead) and deletion endpoint of the tan^2 allele created by hopping the P-element (***A*** of residue 266). (B) Schematic diagram of TAN indicating PEST (a PEST score of +5 or greater is considered significant; Rechsteiner and Rogers, 1996), Basic, and Acidic (AC) domains.

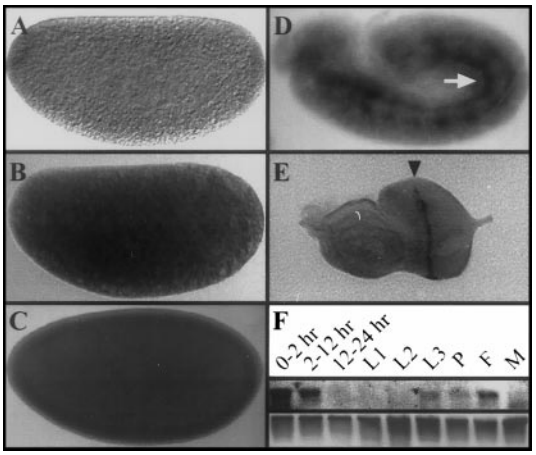

FIG. 3. *In situ* hybridizations and Northern blot. (A) *In situ* hybridization to cleavage stage embryos with a *tan* sense probe. (B–E) *In situ* hybridizations using an anti-sense probe reveals early ubiquitous expression; (B) cleavage stage; (C) cellular blastoderm. (D) During germ band extension, specific expression is seen in the somatic and visceral mesoderm (arrow) in addition to the ubiquitous transcript. For all embryonic stages, anterior is to the left and dorsal up. (E) *tan* expression in an eye-antennal disc: higher expression is seen in the morphogenetic furrow (arrowhead). (F) Developmental Northern analysis of *tan* (top panel). The lower panel shows the same blot stained with Methylene blue as a loading control. Larval (L), Pupal (P), Female (F), and Male (M) stages are indicated.

canonical sites for protein kinase C, cAMP-dependent kinase, and casein kinase II phosphorylation are also present.

Expression of tan

In situ hybridization shows that *tan* transcripts are maternally deposited and uniformly distributed within the egg (Fig. 3). Transcripts are first detected in stage 10 ovaries (not shown) and ubiquitously in precellularized embryos (Figs. 3B and 3C). Transcript levels decrease at cellular blastoderm and then increase once again during germ band extension. At this time, higher levels of expression are seen in what appears to be somatic and visceral mesoderm (Fig. 3D). *tan* is also expressed ubiquitously in imaginal discs of third instar larvae, with higher levels of expression seen in the morphogenetic furrow of the eye-antennal disc (Fig. 3E).

Consistent with these patterns of expression, a developmental Northern (Fig. 3F) shows high levels of *tan* mRNA in early embryos, decreased levels in 12–24 h embryos, and higher levels in third instar larvae and pupae. Females have high levels of expression, as expected for a maternally contributed transcript.

Subcellular Localization of TAN

Polyclonal antibodies were raised against TAN to follow its expression and distribution *in vivo*. This analysis was supplemented by generating transgenic fly lines that express TAN, and a p53 epitope-tagged version of TAN (Dalby and Glover, 1993), under the control of heat shock (HS) and GAL4 inducible promoters. In all assays used, the *tan* and *p53-tan* constructs gave similar results, indicating that the tag has no effect on protein function.

Figure 4A shows that antibodies generated against GST-TAN recognize a *Drosophila* protein that runs with an apparent molecular weight of about 55 kDa. This signal is significantly boosted when extracts are made from HS-*tan* or HS-*p53-tan* fly lines (Fig. 4A). Monoclonal antibodies specific for the p53 epitope tag specifically recognize the induced protein in the p53 transgenic line (Fig. 4A). A protein of similar size was detected in nuclear extracts of

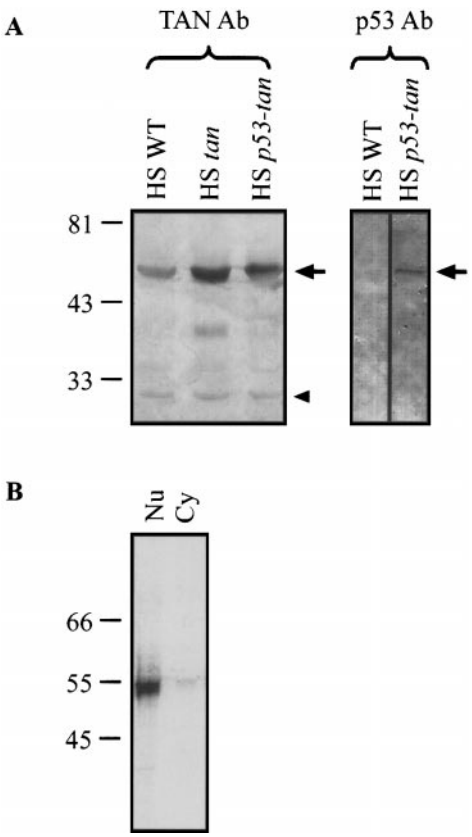

FIG. 4. Western blots. (A) Third instar larval extracts from HS-treated samples incubated with anti-TAN antibodies (first panel). A band of approximately 55 kDa (arrow) is detected in all three lanes and is more abundant in HS-*tan* and HS-*p53-tan* lanes; WT, wild-type. The p53 tag adds 10 amino acids to the protein, resulting in a slower migrating band. The blot was overexposed to demonstrate equal loading (compare cross-reacting bands indicated by arrowhead). A 55-kDa protein is also detected by monoclonal p53 antibodies in HS-*p53-tan* samples, but not in HS-WT samples (second panel). (B) Affinity-purified anti-TAN antibodies detect a 55-kDa protein in Kc cell nuclear (Nu) extracts; Cy, cytoplasmic fraction.

cultured *Drosophila* Kc cells (Fig. 4B), and in reticulocyte lysates following transcription and translation of *tan* mRNA (Fig. 1). Although 55 kDa is significantly larger than the predicted TAN molecular weight (33 kDa), many transcription factors run aberrantly on SDS–PAGE gels (see for example: Krause and Gehring, 1988; Martin and Adler, 1993; Yamamoto *et al.*, 1997).

As ASX acts in the nucleus, and TAN is found in the nucleus of Kc cells (Fig. 4B), it was anticipated that TAN would also exhibit nuclear localization *in vivo*. Affinity-purified TAN antiserum revealed tissue-specific patterns of expression similar to those detected by *in situ* hybridization (data not shown). These levels of expression were not sufficiently strong to determine unambiguously whether TAN localization was nuclear or cytoplasmic. Therefore, untagged and p53-tagged TAN proteins were expressed under heat shock and UAS/GAL4 promoter control to obtain more definitive data. The proteins detected by anti-p53 and anti-TAN antibodies show similar subcellular distributions. Unexpectedly though, this subcellular distribution varies in different tissues. For example, when expressed in stage 11 embryos under *engrailed*-GAL4 control (Fig. 5A) or in imaginal discs using a *patched*-GAL4 driver (Fig. 5B), TAN is clearly enriched in the cytoplasm. However, when expressed in salivary glands or associated fat bodies, the same protein is nuclear (Fig. 5C). These distributions were not tag-dependent and did not change when levels of expression were increased or decreased. Tagged and untagged proteins also exhibited equivalent levels of activity (see below). Additional studies will be required to address the full spectrum of protein distributions in different tissues and stages, and how these distributions affect activity.

Higher magnification of p53-TAN staining in salivary gland nuclei (not shown) suggested association of the protein with the polytene chromosomes. To determine whether endogenous TAN binds discrete loci on polytene chromosomes, affinity-purified anti-TAN antibodies were used to map endogenous protein binding sites. Sixty-six distinct euchromatic binding sites were distinguished (Table 1, and Figs. 5D–5G). More than half of these sites (35/66) overlap in position with previously mapped ASX binding sites (Sinclair *et al.*, 1998a), suggesting that a subset of ASX-regulated loci may be coregulated by TAN. TAN also binds to a number of Polycomb/Polyhomeotic (PC/PH) binding sites not recognized by ASX, indicating that TAN is likely to have functions that are ASX-independent. Somewhat surprisingly, two of the PcG/trxG sites that do not appear to interact with anti-TAN antibodies are those of the BX-C (89E) and ANT-C (84B) homeotic gene clusters (Fig. 5G). This suggests that TAN function is likely to be unrelated to these homeobox gene activities.

Further analysis of the TAN sequence revealed a short stretch of residues within the second basic domain that exhibit homology to the third recognition helix of consensus homeodomain (HD) DNA binding motifs. This suggested the possibility that the association of TAN with

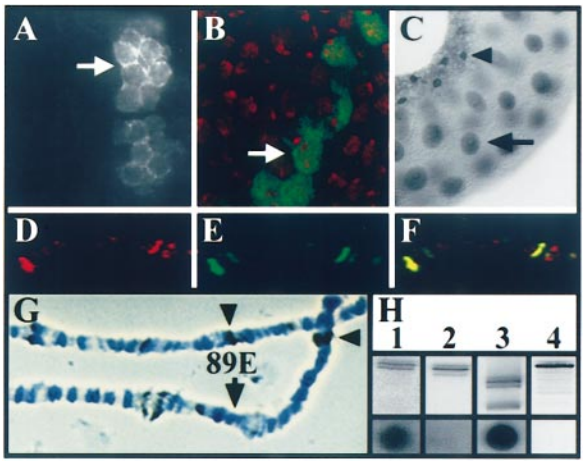

FIG. 5. Subcellular localization of TAN and DNA binding activity. (A) Stage 11 embryo showing cytoplasmic p53-TAN (arrow) expressed under control of an *engrailed*-GAL4 driver and detected by the anti-p53 antibody. (B) Wing imaginal disc showing cytoplasmic nontagged TAN (green; arrow) expressed using a *patched*-GAL4 driver detected by an anti-TAN antibody. Nuclei (red) are stained with propidium iodide. (C) Nuclear p53-TAN expressed in salivary glands (arrow) and fat bodies (arrowhead) under HS promoter control and detected by the anti-p53 antibody. No signal is detected by the anti-p53 antibody in HS-WT tissues (data not shown). (D–F) Colocalization of endogenous ASX (D; red) and TAN (E; green) on a section of salivary gland polytene chromosome from a third instar larva. The merged image (F) shows precise colocalization (yellow) of the two strong bands. (G) Endogenous TAN localization (black) on the third chromosome showing no staining at the site of the BX-C (89E) (arrow). Other strong sites are indicated by arrowheads. Similar results were obtained for the ANT-C. (H) The top series of panels show *in vitro* transcribed and radioactively labeled FTZ (Lane 1), FTZΔHD (Lane 2), TAN (Lane 3), and LUC (Lane 4) proteins analyzed by SDS–PAGE. Bottom panels show the ability of each protein to bind salmon sperm DNA blotted to a filter. TAN and FTZ bind strongly while FTZΔHD and LUC do not.

specific sites on polytene chromosomes may depend, in part, on its own ability to bind DNA. To test this possibility, ^{35}S-labeled TAN was incubated with salmon sperm DNA previously bound to nitrocellulose filters (Fig. 5H). The Fushi tarazu protein, with (FTZ) and without (FTZΔHD) its DNA binding homeodomain, and Luciferase (LUC), which does not bind DNA, were used as controls. Of the four polypeptides, TAN yielded the strongest signal. Full-length FTZ also bound to the blotted DNA, and, as expected, FTZΔHD and LUC both failed to bind. Thus, TAN has a general ability to bind DNA. The testing of sequence-specific DNA binding properties awaits the development of an expression system capable of expressing suitable amounts of intact protein. Full-length TAN is rapidly degraded when expressed in bacteria.

TABLE 1
Polytene Chromosome Binding Sites for TAN, with those that bind ASX and PC/PH Indicated

X		3*L*	
1D	ASX	61F	ASX, PC/PH
3D		62F	ASX, PC/PH
6A		63A	ASX
8A	ASX, PC/PH	64A	PC/PH
9CD		64C	ASX
10F		65B	
13E	ASX, PC/PH	66A	ASX
19D	ASX, PC/PH	67D	ASX, PC/PH
		68C	
2*L*		70A	ASX, PC/PH
		70D	ASX, PC/PH
21A	ASX, PC/PH	72EF	
24A	ASX, PC/PH	74EF	
25EF	ASX, PC/PH	75F	
27B	ASX	80A	
29E	PC/PH		
30A	ASX	3*R*	
33C			
34A	PC/PH	82C	
34D	PC/PH	84D	ASX, PC/PH
35A	ASX, PC/PH	84F	ASX, PC/PH
37D	ASX	85D	ASX
38D	ASX	86C	ASX, PC/PH
39EF	ASX, PC/PH	87EF	PC/PH
		88C	
2*R*		88F	
		89A	
41C	ASX, PC/PH	89B	ASX, PC/PH
42B		91D	
42D		92C	
44C		93E	ASX, PC/PH
46A	ASX	94D	PC/PH
47C		95A	
48A	ASX, PC/PH	96A	ASX
50A	ASX	97E	
52E		98C	ASX, PC/PH
56D	ASX		
58CD	PC/PH		
59F	ASX, PC/PH		

Mutagenesis of the tan Gene

In situ hybridization to polytene chromosomes and the screening of a P1 phage library show that *tan* is located at 65A on chromosome 3 (data not shown). Since no candidate *tan* mutations were located in this region, P-element mutagenesis was used to generate *tan* alleles. Three P-element lines that map in the 65A region (Deák *et al.,* 1997) were obtained and mobilized to generate 270 new lines (see Materials and Methods). Using PCR, one of the mobilized elements (referred to hereafter as tan^1) was found to have inserted upstream of the *tan* translation start site (see Fig. 2A). A null allele of *tan* was then generated by mobilizing the tan^1 P-element and using PCR to screen for imprecise excisions of the *tan* gene. A 1.4-kb deletion was identified that removes sequences in the 3′ direction only. This deletion removes 266 of the 299 encoded TAN residues (see Fig. 2A). Southern blotting and additional PCR controls (data not shown) confirm the deletion and show that no duplications of the gene occurred during the course of mutagenesis. This deficiency allele of *tan* is referred to hereafter as tan^2.

tan Mutant Phenotypes

Despite the fact that *tan* is widely expressed during much of development, tan^2 flies, which have the majority of the gene deleted, are homozygous viable and fertile (as are their progeny). Examination of both tan^1 and tan^2 homozygous adults (unless stated otherwise, tan^1 and tan^2 mutants described from hereon are homozygous), however, revealed a number of morphological defects. These include a rough-eye phenotype, the loss or duplication of sensory bristles, and shortened veins in the wings. A common feature of each of these tissues is that they comprise or contain enervated sensory organs. These defects are discussed further below.

Consistent with the expression of *tan* in the eye-antennal disc, *tan* mutants have a rough eye appearance due to ommatidia defects and the deletion or duplication of ommatidial bristles (Figs. 6B and 6D). Wild-type ommatidia have a uniform size and hexagonal appearance with bristles equally spaced at three of the six corners (Figs. 6A and 6C). In contrast, a high percentage of *tan* mutant ommatidia are smaller with some deleted altogether or fused with neighbors (Fig. 6D). Bristles are frequently paired together or missing. These defects suggest developmental errors in both photoreceptor and bristle-forming cell lineages.

In wild-type flies, the medial part of the adult head contains three additional light-sensitive organs called ocelli with numerous sensory bristles spaced around (macrochaetae) and between (microchaetae) them (Fig. 6E). In tan^2 mutants, the number of microchaetae between the ocelli decreases from an average of 8 ($\pm$2) seen in wild-type flies to 5 ($\pm$2) (Fig. 6F, and Table 2). *tan* mutants also exhibit macrochaetae duplications (predominantly scutellar bristles; 8% of flies), and abdominal sternites and tergites occasionally exhibit smaller, irregularly spaced, and/or ectopic bristles (data not shown). Finally, the fifth wing vein fails to reach the posterior wing margin in 85% of tan^2 flies (Fig. 6G, and Table 2).

These tan^2 phenotypes are fully or partially rescued by two copies of a genomic *tan* rescue construct (P[*tan*]; Table 2, and data not shown) which contains 1.4 kb of upstream sequence and 3 kb of downstream sequence, verifying that the phenotypes described are directly attributable to the *tan* mutations tested. To further confirm *tan* mutations as the cause of the defects described above, tan^2 was crossed to a deletion that uncovers the 65A region (Table 2, and data not shown). These hemi-

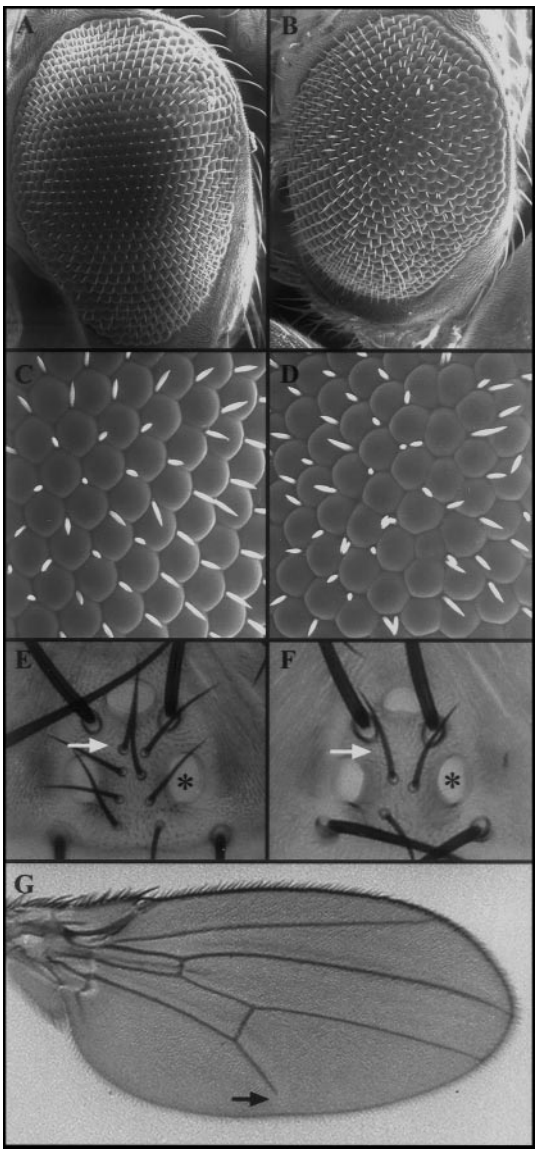

FIG. 6. *tan*^{2} homozygous mutant phenotypes. Scanning electron micrographs of adult eyes at low (A, B) and high (C, D) magnifications; (A, C) wild-type; (B, D) *tan*^{2} mutants. Notice the rough appearance due to disruption of ommatidial spacing and the misplaced, duplicated, or missing bristles. Flies were raised at 30°C. (E) Wild-type dorsal head with one of the three ocelli indicated by an asterisk and interocellar bristles indicated by arrow (anterior is up). The larger ocellar bristles (top) and postvertical bristles (bottom) are also visible. (F) A *tan*^{2} homozygous mutant with only three interocellar bristles (arrow). (G) *tan*^{2} mutant wing showing a fifth vein which does not reach the margin (arrow).

zygous flies display phenotypes with similar frequencies and severities to those of homozygous *tan*^{2} mutants. We conclude that *tan*^{2} is most likely a null allele and the sole cause of the defects observed.

Developmental Defects Caused by Ectopic TAN Expression

tan and *p53-tan* were expressed under the control of different promoters to determine whether ectopic expression might induce additional developmental defects that shed further light on the function of the protein. As a first approach, the genomic *tan* rescue construct was introduced into wild-type flies to double the gene copy from two to four. These flies were viable but exhibited defects in a variety of sensory tissues. For example, of the two lines generated, one (Line A) showed deletions of the macrochaetae referred to as postvertical bristles, located just posterior to the ocelli (Fig. 7A). The second line (Line B) had a more variable effect on these bristles, including reductions in size (Fig. 7B), occasional deletions with sockets remaining (Fig. 7C), and rare deletions where the sockets were also missing, similar to Line A. This graded effect suggests that *tan* may function at different stages of bristle specification, and that the level of *tan* activity is important for these functions. HS-*tan* and HS-*p53-tan* lines reared at 30°C to induce low levels of *tan* expression also had frequent deletions of the postvertical bristles (up to 40% of the flies had one or both bristles missing).

To test the effects of ectopic expression, the UAS-*tan* and UAS-*p53-tan* constructs described earlier were expressed under the control of various GAL4 drivers. Expression of either the tagged or untagged protein under the control of a *patched*-GAL4 driver yielded viable adults with similar but stronger bristle phenotypes than those seen with extra copies of the gene. Most bristles in the ocellar and scutellar regions were frequently missing (Fig. 7D). In contrast, expression under the control of a *hairy*-GAL4 driver caused pupal lethality. When grown at 18°C, however, occasional escapers could be recovered from one of the two lines. These flies were weakly viable and, in addition to other phenotypes, showed ectopic wing veins or wing vein material (not shown). Similar wing vein hypertrophies were

TABLE 2

Analysis of Selected *tan* Mutant and Rescued Phenotypes

	Interocellar bristles (%)[a]	Wing vein (%)[b]
tan^2/*tan*^{2}	36.7 (387)	85.1 (174)
P[*tan*]/P[*tan*]; *tan*^{2}/*tan*^{2}	0 (357)	30.8 (120)
CH4/*tan*^{2}	40.4 (383)	—
TM3, Sb/*tan*^{2}	3.4 (357)	—

Note. The percent of flies that displayed the indicated phenotypes and the number of flies analyzed (in brackets) are shown for each cross. P[*tan*] is the genomic rescue construct, CH4 is a deletion of 64E-65B1, 2, and TM3, Sb is a balancer chromosome. For the CH4/TM3, Sb–containing cross, reciprocal matings were performed and, as the results did not vary, the data were pooled.

[a] Flies with four or fewer interocellar bristles.

[b] Flies with a shortened fifth wing vein.

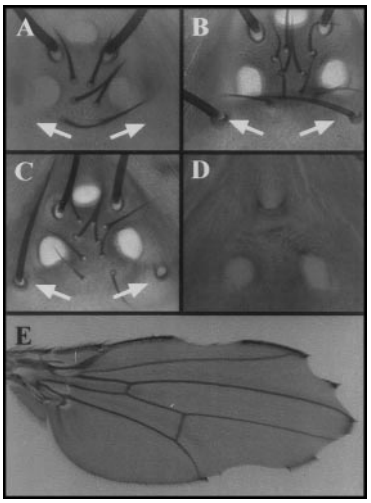

FIG. 7. Ectopic and over expression of *tan* disrupts sensory lineages. (A) Post-vertical bristles (arrows) are frequently deleted in Line A flies (4 copies of *tan*). (B, C) Line B flies (4 copies of *tan*) showing either smaller postvertical bristles (B) (compare left and right bristles indicated by arrows), or deletions of the bristle but not the socket (C). (D) A UAS-*p53-tan* line driven by *patched*-GAL4 has all bristles in the occellar region missing, while the occelli and cuticle are unaffected. (E) A wing from a fly expressing *tan* under control of the wing disk-specific GAL4 driver C96.

observed with one of the lines carrying four copies of endogenous *tan*. Interestingly, when using the wing-specific C96 driver, which expresses along the wing margin, wings were heavily notched (Fig. 7E). These results provide further support for *tan* playing a specific role in the differentiation of sensory lineages. The lethality caused by certain GAL4 drivers suggests that processes in addition to those revealed by *tan* null mutants are under *tan* control.

Asx and tan Interact Genetically

To test whether ASX and TAN act together to control sensory organ specification, *Asx* and *tan* mutants were combined and *tan* bristle phenotypes scored. We focused on the highly penetrant and well characterized loss of interocellar bristles phenotype. To ensure a stringent assessment, only flies with four or fewer interocellar bristles were scored.

To determine whether *Asx* plays a role in bristle specification, we first crossed several *Asx* gain-of-function (GOF) alleles (Sinclair *et al.*, 1992) to *tan* mutant flies. The Asx^{15} and Asx^{9} alleles both strongly suppressed the *tan* interocellar bristle phenotype (Table 3). Because these alleles were made in the same background, we also tested another GOF allele, Asx^{3}, and found that it too rescued the *tan*-induced bristle phenotype (Table 3).

Additionally, the loss-of-function (LOF) *Asx* allele, Df(2R)*trix*, was crossed to *tan* mutants. Interestingly, in this particular background, the *tan* phenotype on its own is significantly reduced (only 2–5% of *CyO; tan* flies versus 37% of tan^{2} homozygous flies exhibit reduced numbers of bristles). Although the basis of this modifier effect is unknown, it has been observed previously with this particular *Asx* allele and genetic background (see Table 2 in Milne *et al.*, 1999). Despite this decreased penetrance, the combination of Df(2R)*trix* and *tan* significantly enhances the penetrance of the *tan* bristle phenotype (from ~2 to 15%; Table 3). To confirm this genetic enhancement, the genomic *tan* rescue line was crossed to Df(2R)*trix*/CyO; tan^{2}/tan^{2} flies. Introduction of one copy of P[*tan*] completely rescues the *tan* bristle phenotype in CyO progeny and rescues the *tan* component of the bristle phenotype in Df(2R)*trix;* tan^{2}/tan^{2} siblings (Table 3). To further verify that the Df(2R)*trix* allele affects bristle specification, we out-crossed this allele to control flies. Seven percent (n = 167) of the heterozygous Df(2R)*trix* progeny exhibited the bristle phenotype, while all control siblings were wild-type (n = 88), demonstrating that the Df(2R)*trix* allele affects interocellar bristle specification.

Asx mutants produce homeotic defects, including ectopic sex combs on the T2 legs of males. These transformations were not enhanced by the presence of *tan*, nor did deletions of *tan* alter the expression patterns of the homeotic genes *Antennapedia*, *Ultrabithorax*, or *Sex combs reduced* (data not shown), consistent with our inability to detect binding of TAN at the sites of the ANT-C and BX-C on polytene chromosomes. Thus, *tan* appears to have no role in the regulation of HOM-C genes.

TABLE 3

tan and *Asx* Interact Genetically in Interocellar Bristle Specification

Mutant allele	CyO/+; *tan/tan* (%)	*Asx*/+; *tan/tan* (%)	CyO/P[*tan*]; *tan/tan* (%)	*Asx*/P[*tan*]; *tan/tan* (%)
Asx^{15}	26.0 (292)	4.4 (475)	—	—
Asx^{9}	25.9 (255)	7.0 (440)	—	—
Asx^{3}	9.3 (400)	6.0 (465)	—	—
Asx^{3}*	18.8 (256)	6.3 (286)	—	—
Df(2R)*trix*	1.7 (301)	15.0 (381)	0 (376)	1.5 (464)
Df(2R)*trix**	4.6 (241)	16.9 (313)	—	—

Note. Crosses were *Asx*/CyO; tan^{2}/tan^{2} females to tan^{2}/tan^{2} males, except *, which were *Asx*/CyO; tan^{1}/tan^{1} females to tan^{1}/tan^{1} males. *Asx*/+; *tan/tan* and CyO/+; *tan/tan* siblings were then compared (columns 2 and 3). Df(2R)*trix*/CyO; tan^{2}/tan^{2} females were also crossed to P[*tan*]/P[*tan*]; tan^{2}/tan^{2} males to rescue the interocellar bristle phenotype associated with the *tan* mutation (columns 4 and 5). Values indicate the percentage of flies with four or fewer interocellar bristles, with the number of flies counted in brackets. All crosses were repeated twice, except for those crosses involving the tan^{1} allele, and the data pooled. Results were verified for significance by χ^{2} analysis (α = 0.05).

DISCUSSION

TAN, a New ASX Cofactor

A major objective of this study was to identify ASX-interacting proteins that might help explain the tissue-specific activities of ASX (Soto *et al.*, 1995). Such tissue-specificity could result from many different mechanisms, including tissue-specific regulation of the *Asx* promoter, tissue-specific expression of other PcG/trxG proteins, or through the actions of yet to be identified cofactors. Since *Asx* does not appear to be expressed in tissue-specific patterns, it was speculated that tissue-specific cofactors were likely to exist (Soto *et al.*, 1995; Sinclair *et al.*, 1998a).

TAN was identified as an ASX-interacting protein by using a yeast two-hybrid screen, and the interaction was confirmed by a GST pull-down assay. TAN shows no extended regions of homology to other proteins currently listed in the databases but does feature several general properties typical of transcription factors. These include stretches of basic residues, consensus nuclear localization motifs, and a short motif found in other DNA binding proteins. Consistent with these properties, TAN binds DNA *in vitro*, is enriched in the nucleus in a subset of tissues, and associates with 66 sites on polytene chromosomes.

TAN also displays properties that are consistent with it being an important cofactor for ASX. It associates with ASX in yeast and *in vitro*, colocalizes with ASX at 35 of 66 TAN chromosomal binding sites, and interacts genetically with *Asx in vivo*. The ability of TAN to bind DNA *in vitro* suggests a possible role in recruiting or anchoring ASX-containing complexes to specific sites on DNA.

ASX and TAN Are Involved in Sensory Organ Development

Most members of the PcG and trxG protein complexes characterized thus far associate with both the ANT-C and BX-C gene clusters and cause homeotic transformations when mutated. However, TAN appears to have no role in the regulation of these genes. Rather, TAN appears to play a specific role in the differentiation of sensory tissues. Our data show that ASX is also required in at least a subset of these tissues, and that when *tan* and *Asx* mutations are combined, these sensory organ defects are specifically enhanced or suppressed. Taken together, these results suggest that TAN acts as a tissue-specific ASX cofactor in sensory tissue differentiation. Further work will be required to determine whether ASX acts together with TAN to coregulate all other *tan*-dependent processes. This need not be the case, as ASX only colocalizes to 35/66 mapped TAN polytene chromosome binding sites.

Although the majority of PcG and trxG components identified to date were isolated via genetic screens for the suppression or enhancement of homeotic transformations, loss of sensory bristle phenotypes have been observed when other trxG/PcG genes are misexpressed. Examples include loss-of-function mutations in the trxG genes *brahma* (Elfring *et al.*, 1998), *absent, small,* or *homeotic disks2* (Adamson and Shearn, 1996), *leg arista wing complex* (Zorin *et al.*, 1999), and *Asx* (this study). Loss of bristle phenotypes are also observed after ectopic expression of the trxG gene *osa* (Collins *et al.*, 1999) and the PcG genes *Posterior sex combs* and *Suppressor 2 of Zeste* (Sharp *et al.*, 1994). Additional studies will be required to determine which bristle genes TAN and ASX are acting through, and whether this regulation is positive or negative in nature.

The defects in sensory organ tissues caused by *tan* misexpression are remarkably similar to those caused by mutations in the *Notch* (*N*) gene (see Lindsley and Zimm, 1992). Consistent with a possible intersection between TAN and N functions, we find that *N* mutations specifically and strongly enhance the *tan* interocellar bristle phenotype (B.H.D. and H.M.K., unpublished observations). Numerous studies have shown that *N* is required at two different stages of sensory organ development, during specification of the sensory organ precursor (SOP) cells and during the subsequent specification of SOP daughter cells (reviewed in Artavanis-Tsakonas *et al.*, 1999). The ability of TAN to cause similar defects suggests that it is also involved during both stages of bristle development.

TAN Subcellular Localization

An interesting feature of TAN that has not previously been noted for other trxG or PcG complex components is that its subcellular localization varies in a tissue-specific manner. In embryos, protein expressed using the GAL4 system is primarily cytoplasmic, while, in third instar larvae, it is cytoplasmically enriched in some tissues and nuclearly in others. Although the mechanism and importance of this localization have yet to be addressed, it suggests a novel means of functional regulation.

To date, the number of transcription factors known to cycle between cytoplasm and nucleus are relatively few. Other well-characterized examples include proteins such as Dorsal, Arm/β-catenin, STAT proteins, MAD proteins, and components of the Notch signaling pathway, including N itself (reviewed in Weinmaster, 2000). The latter example is particularly notable, given the genetic interaction between *N* and *tan* described above.

Control of TAN nuclear localization may partially explain the restriction of mutant phenotypes to sensory lineages, despite fairly ubiquitous patterns of gene expression. Retention in the cytoplasm may be a general way of relegating TAN activity to a subset of TAN-expressing

cells. On the other hand, the cytoplasmically localized protein may also serve a function that has yet to be elaborated.

Other Roles of TAN

The majority of *Drosophila* genes remaining to be genetically characterized, like *tan*, appear to be nonessential for viability. A major reason for this is likely to be overlap or redundancy between gene functions. Thus, the relatively modest nature of *tan* mutant phenotypes, despite prolonged and widespread expression of the gene, may also be explained by redundancy. Several observations lend weight to this argument. First, *tan* bristle phenotypes are highly variable in terms of penetrance and severity, and can be enhanced further by shifts in temperature. Second, lethal phenotypes are induced by ectopic or overexpression. Third, more than half of the TAN polytene chromosome binding sites do not appear to colocalize with ASX. The mapped TAN binding sites also show heterogeneity with respect to other PcG/trxG protein binding sites. This heterogeneity of protein complexes at different loci suggests the likelihood of different functions and outputs for each protein complex. Revealing the full extent of these TAN complex activities will likely require elimination of the redundantly acting factors.

ACKNOWLEDGMENTS

We thank Carl Hashimoto, Kathy Matthews and the Umea Stock Center for fly stocks, Shelley Lumba for assistance with antibody characterization, and Howard Lipshitz for comments on the manuscript. This work was supported by funds provided by the Canadian Institutes of Health Research (to H.M.K. and H.W.B.), the Natural Sciences and Engineering Research Council (to H.W.B.) and a University of Toronto Open Fellowship (to B.H.D.). *tan* sequence data has been submitted to the DDBJ/EMBL/GenBank databases under accession number AF218585.

REFERENCES

Adamson, A.L., and Shearn, A. (1996). Molecular genetic analysis of *Drosophila ash2*, a member of the trithorax group required for imaginal disc pattern formation. *Genetics* **144,** 621–633.

Artavanis-Tsakonas, S., Rand, M. D., and Lake, R. J. (1999). Notch signaling: Cell fate control and signal integration in development. *Science* **284,** 770–776.

Brand, A. H., and Perrimon, N. (1993). Targeted gene expression as a means of altering cell fates and generating dominant phenotypes. *Development* **118,** 401–415.

Breen, T. R., and Duncan, I. M. (1986). Maternal expression of genes that regulate the bithorax complex of *Drosophila melanogaster*. *Dev. Biol.* **118,** 442–456.

Campbell, R. B., Sinclair, D. A., Couling, M., and Brock, H. W. (1995). Genetic interactions and dosage effects of *Polycomb* group genes of. *Drosophila Mol. Gen. Genet.* **246,** 291–300.

Cavener, D. R. (1987). Comparison of the consensus sequence flanking translational start sites in *Drosophila* and vertebrates. *Nucleic Acids Res.* **15**, 1353–1361.

Collins, R. T., Furukawa, T., Tanese, N., and Treisman, J. E. (1999). Osa associates with the Brahma chromatin remodeling complex and promotes the activation of some target genes. *EMBO J.* **18,** 7029–7040.

Crosby, M. A., Miller, C., Alon, T., Watson, K. L., Verrijzer, C. P., Goldman-Levi, R., and Zak, N. B. (1999). The *trithorax* group gene *moira* encodes a brahma-associated putative chromatin-remodelling factor in *Drosophila melanogaster*. *Mol. Cell. Biol.* **19**, 1159–1170.

Dalby, B., and Glover, D. M. (1993). Discrete sequence elements control posterior pole accumulation and translational repression of maternal cyclin B RNA in *Drosophila*. *EMBO J.* **12**, 1219–1227.

Deák, P., Omar, M. M., Saunders, R. D., Pal, M., Komonyi, O., Szidonya, J., Maroy, P., Zhang, Y., Ashburner, M., Benos, P., Savakis, C., Siden-Kiamos, I., Louis, C., Bolshakov, V. N., Kafatos, F. C., Madueno, E., Modolell, J., and Glover, D. M. (1997). P-element insertion alleles of essential genes on the third chromosome of *Drosophila melanogaster*: Correlation of physical and cytogenetic maps in chromosomal region 86E–87F. *Genetics* **147,** 1697–1722.

DeCamillis, M., Cheng, N. S., Pierre, D., and Brock, H. W. (1992). The *polyhomeotic* gene of *Drosophila* encodes a chromatin protein that shares polytene chromosome-binding sites with. *Polycomb*. *Genes Dev.* **6,** 223–232.

Dingwall, A. K., Beek, S. J., McCallum, C. M., Tamkun, J. W., Kalpana, G. V., Goff, S. P., and Scott, M. P. (1995). The *Drosophila* snr1 and brm proteins are related to yeast SWI/SNF proteins and are components of a large protein complex. *Mol. Biol. Cell* **6,** 777–791.

Elfring, L. K., Daniel, C., Papoulas, O., Deuring, R., Sarte, M., Moseley, S., Beek, S. J., Waldrip, W. R., Daubresse, G., DePace, A., Kennison, J. A., and Tamkun, J. W. (1998). Genetic analysis of brahma: The *Drosophila* homolog of the yeast chromatin remodeling factor SWI2/SNF2. *Genetics* **148,** 251–265.

Franke, A., DeCamillis, M., Zink, D., Cheng, N., Brock, H. W., and Paro, R. (1992). *Polycomb* and *polyhomeotic* are constituents of a multimeric protein complex in chromatin of *Drosophila melanogaster*. *EMBO J.* **11,** 2941–2950.

Gildea, J. J., Lopez, R., and Shearn, A. (2000). A screen for new Trithorax Group genes identified *little imaginal discs*, the *Drosophila melanogaster* homologue of Human Retinoblastoma Binding Protein 2. *Genetics* **156,** 645–663.

Gunster, M. J., Satijn, D.P.E., Hamer, K. M., den Blaauwen, J. L., de Bruijn, D., Alkema, M. J., van Lohuizen, M., van Driel, R., and Otte, A. P. (1997). Identification and characterization of interactions between the vertebrate Polycomb-group protein BMI1 and human homologs of Polyhomeotic. *Mol. Cell. Biol.* **17,** 2326–2335.

Hamilton, B. A., and Zinn, K. (1994). From clone to mutant gene. In "Methods in Cell Biology: *Drosophila melanogaster*: Practical Uses in Cell and Molecular Biology" (L. S. B Goldstein and E. A. Fyrberg, Eds.), Vol. 44, pp. 81–94. Academic Press, San Diego.

Hashimoto, N., Brock, H. W., Nomura, M., Kyba, M., Hodgson, J.,

Fujita, Y., Takihara, Y., Shimada, K., and Higashinakagawa, T. (1998). RAE28, BMI1 and M33 are members of heterogeneous multimeric mammalian Polycomb group complexes. *Biochem. Biophys. Res. Commun.* **245,** 356–365.

Hughes, S. C., and Krause, H. M. (1999). Single and Double FISH protocols for *Drosophila*. In "Methods in Molecular Biology: Confocal Microscopy Methods and Protocols" (S.W. Paddock, Ed.), Vol. 122, pp. 93–101. Humana Press, Totowa, NJ.

Jacobs, J. J. L., and van Lohuizen, M. (1999). Cellular memory of transcriptional states by Polycomb-group proteins. *Cell Dev. Biol.* **10,** 227–235.

Jones, C. A., Ng, J., Peterson, A. J., Morgan, K., Simon, J., and Jones, R. S. (1998). The *Drosophila* esc and E(z) proteins are direct partners in polycomb group-mediated repression. *Mol. Cell. Biol.* **18,** 2825–2834.

Jürgens, G. (1985). A group of genes controlling the spatial expression of the bithorax complex in *Drosophila. Nature* **316**, 153–155.

Kal, A. J., Mahmoudi, T., Zak, N. B., and Verrijzer, P. C. (2000). The *Drosophila* Brahma complex is an essential coactivator for the *trithorax* group protein Zeste. *Genes Dev.* **14,** 1058–1071.

Kennison, J. A., and Tamkun, J. W. (1988). Dosage-dependent modifiers of *polycomb* and *antennapedia* mutations in *Drosophila. Proc. Nat. Acad. Sci. USA* **85**, 8136–8140.

Kennison, J. A. (1995). The Polycomb and trithorax group proteins of *Drosophila*: trans-regulators of homeotic gene function. *Annu. Rev. Genet.* **29,** 289–303.

Klemenz, R., Weber, U., and Gehring, W. J. (1987). The *white* gene as a marker in a new P-element vector for gene transfer in *Drosophila. Nucleic Acids Res.* **15**, 3947–3959.

Krause, H. M., and Gehring, W. J. (1988). The location, modification, and function of the *fushi tarazu* protein during *Drosophila* embryogenesis. In "Cellular Factors in Development and Differentiation: Embryos, Teratocaricinomas, and Differentiated Tissues" (S. Harris and P. E. Mansson, Eds.), pp. 105–123. A. R. Liss, New York.

Kyba, M., and Brock, H. W. (1998). The *Drosophila* polycomb group protein Psc contacts ph and Pc through specific conserved domains. *Mol. Cell. Biol.* **18,** 2712–2720.

LaJeunesse, D., and Shearn, A. (1996). *E(z)*: A polycomb group gene or a trithorax group gene? *Development* **122** 2189–2197.

Landecker, H. L., Sinclair, D.A.R., and Brock, H. W. (1994). A screen for enhancers of *Polycomb* and *Polycomblike* in *Drosophila melanogaster. Dev. Genet.* **15,** 425–434.

Lindsley, D. L., and Zimm, G. G. (1992). "The Genome of *Drosophila melanogaster.* " Academic Press, San Diego.

Lonie, A., D'Andrea, R., Paro, R., and Saint, R. (1994). Molecular characterisation of the *Polycomblike* gene of *Drosophila melanogaster,* a trans-acting negative regulator of homeotic gene expression. *Development* **120,** 2629–2636.

Manoukian, A. S., and Krause, H. M. (1992). Concentration-dependent activities of the *even-skipped* protein in *Drosophila* embryos. *Genes and Dev.* **6**, 1740–1751.

Martin, E. C., and Adler, P. N. (1993). The *Polycomb* group gene *Posterior Sex Combs* encodes a chromosomal protein. *Development* **117,** 641–655.

McKeon, J., and Brock, H. W. (1991). Interactions of the *Polycomb* group of genes with homeotic loci of *Drosophila. Roux's Arch. Dev. Biol.* **199,** 387–396.

Milne, T. A., Sinclair, D. A., and Brock, H. W. (1999). The *Additional sex combs* gene of *Drosophila* is required for activation and repression of homeotic loci, and interacts specifically with *Polycomb and super sex combs. Mol. Gen. Genet.* **261,** 753–761.

Nüsslein-Volhard, C., Weischaus, E., and Kluding, H. (1984). Mutations affecting the pattern of the larval cuticle in *Drosophila melanogaster* I. Zygotic loci on the second chromosome. *Roux's Arch. Dev. Biol.* **193,** 267–282.

Papoulas, O., Beek, S. J., Moseley, S. L., McCallum, C. M., Sarte, M., Shearn, A., and Tamkun, J. W. (1998). The *Drosophila* trithorax group proteins BRM, ASH1 and ASH2 are subunits of distinct protein complexes. *Development* **125,** 3955–3966.

Paro, R. (1990). Imprinting a determined state into the chromatin of *Drosophila. Trends Genet.* **6,** 416–421.

Peterson, A. J., Kyba, M., Bornemann, D., Morgan, K., Brock, H. W., and Simon, J. (1997). A domain shared by the Polycomb group proteins Scm and ph mediates heterotypic and homotypic interactions. *Mol. Cell. Biol.* **17,** 6683–6692.

Rastelli, L., Chan, C. S., and Pirrotta, V. (1993). Related chromosome binding sites for *zeste*, suppressors of *zeste* and *Polycomb* group proteins in *Drosophila* and their dependence on *Enhancer of zeste* function. *EMBO J.* **12**, 1513–1522.

Rechsteiner, M., and Rogers, S. W. (1996). PEST sequences and regulation by proteolysis. *Trends Biochem. Sci.* **21,** 267–271.

Sambrook, J., Fritsch, E. F., and Maniatis, T. (1989). "Molecular Cloning: A Laboratory Manual, 2nd edition." Cold Spring Harbor Laboratory Press, Cold Spring Harbor, New York.

Shao, Z., Raible, F., Mollaaghababa, R., Guyon, J. R., Wu, C. T., Bender, W., and Kingston, R. E. (1999). Stabilization of chromatin structure by PRC1, a Polycomb complex. *Cell* **98,** 37–46.

Sharp, E. J., Martin, E. C., and Adler, P. N. (1994). Directed overexpression of *suppressor 2 of zeste* and *Posterior Sex Combs* results in bristle abnormalities in *Drosophila melanogaster. Dev. Biol.* **161**, 379–392.

Simon, J., Chiang, A., and Bender, W. (1992). Ten different *Polycomb* group genes are required for spatial control of the *abdA* and *AbdB* homeotic products. *Development* **114,** 493–505.

Simon, J. (1995). Locking in stable states of gene expression: Transcriptional control during *Drosophila* development. *Curr. Opin. Cell Biol.* **7,** 376–385.

Sinclair, D. A., Campbell, R. B., Nicholls, F., Slade, E., and Brock, H. W. (1992). Genetic analysis of the *Additional sex combs* locus of *Drosophila melanogaster. Genetics* **130,** 817–825.

Sinclair, D. A., Milne, T. A., Hodgson, J. W., Shellard, J., Salinas, C. A., Kyba, M., Randazzo, F., and Brock, H. W. (1998a). The *Additional sex combs* gene of *Drosophila* encodes a chromatin protein that binds to shared and unique Polycomb group sites on polytene chromosomes. *Development* **125,** 1207–1216.

Sinclair, D. A., Clegg, N. J., Antonchuk, J., Milne, T. A., Stankunas, K., Ruse, C., Grigliatti, T. A., Kassis, J. A., and Brock, H. W. (1998b). *Enhancer of Polycomb* is a suppressor of position-effect variegation in *Drosophila melanogaster. Genetics* **148**, 211–220.

Soto, M. C., Chou, T. B., and Bender, W. (1995). Comparison of germline mosaics of genes in the Polycomb group of *Drosophila melanogaster. Genetics* **140,** 231–243.

Strutt, H., and Paro, R. (1997). The Polycomb Group protein complex of *Drosophila melanogaster* has different compositions at different target genes. *Mol. Cell. Biol.* **17,** 6773–6783.

Thummel, C. S., and Pirrotta, V. (1992). New pCaSpeR P-element vectors. *Drosophila Inf. Serv.* **71,** 150.

Tie, F., Furuyama, T., and Harte, P. J. (1998). The *Drosophila* Polycomb Group proteins ESC and E(Z) bind directly to each other and co-localize at multiple chromosomal sites. *Development* **125,** 3483–3496.

Weinmaster, G. (2000). Notch signal transduction: A real Rip and more. *Curr. Opin. Genet. Dev.* **10,** 363–369.

Yamamoto, Y., Girard, F., Bello, B., Affolter, M., and Gehring, W. J. (1997). The *cramped* gene of *Drosophila* is a member of the *Polycomb*-group, and interacts with *mus209*, the gene encoding Proliferating Cell Nuclear Antigen. *Development* **124,** 3385–3394.

Zink, B., and Paro, R. (1989). In vivo binding pattern of a trans-regulator of homoeotic genes in *Drosophila melanogaster*. *Nature* **337**, 468–471.

Zorin, I. D., Gerasimova, T. I., and Corces, V. G. (1999). The *lawc* gene is a new member of the trithorax-group that affects the function of the gypsy insulator of *Drosophila*. *Genetics* **152,** 1045–1055.

Submitted for publication January 24, 2001
Revised February 26, 2001
Accepted February 28, 2001
Published online May 1, 2001